Molecular Cell
Article

The Histone H3 Lysine 9 Methyltransferases G9a and GLP Regulate Polycomb Repressive Complex 2-Mediated Gene Silencing

Chiara Mozzetta,[1,6,*] Julien Pontis,[1,6] Lauriane Fritsch,[1] Philippe Robin,[1] Manuela Portoso,[3,4,5] Caroline Proux,[2] Raphaël Margueron,[3,4,5] and Slimane Ait-Si-Ali[1,*]
[1]Université Paris Diderot, Sorbonne Paris Cité, Laboratoire Epigénétique et Destin Cellulaire, UMR7216, Centre National de la Recherche Scientifique CNRS, 35 rue Hélène Brion, 75013 Paris, France
[2]Institut Pasteur, PF2 Plate-forme Transcriptome et Epigénome, 28 rue du Dr Roux, Paris, 75015 France
[3]Institut Curie, 26 rue d'Ulm, 75005 Paris, France
[4]UMR3215 CNRS, 26 rue d'Ulm, 75005 Paris, France
[5]U934 INSERM, 26 rue d'Ulm, 75005 Paris, France
[6]These authors contributed equally to this work
*Correspondence: chiara.mozzetta@univ-paris-diderot.fr (C.M.), slimane.aitsiali@univ-paris-diderot.fr (S.A.)
http://dx.doi.org/10.1016/j.molcel.2013.12.005

SUMMARY

G9a/GLP and Polycomb Repressive Complex 2 (PRC2) are two major epigenetic silencing machineries, which in particular methylate histone H3 on lysines 9 and 27 (H3K9 and H3K27), respectively. Although evidence of a crosstalk between H3K9 and H3K27 methylations has started to emerge, their actual interplay remains elusive. Here, we show that PRC2 and G9a/GLP interact physically and functionally. Moreover, combining different genome-wide approaches, we demonstrate that Ezh2 and G9a/GLP share an important number of common genomic targets, encoding developmental and neuronal regulators. Furthermore, we show that G9a enzymatic activity modulates PRC2 genomic recruitment to a subset of its target genes. Taken together, our findings demonstrate an unanticipated interplay between two main histone lysine methylation mechanisms, which cooperate to maintain silencing of a subset of developmental genes.

INTRODUCTION

Eukaryotic genomes are tightly packed around octamers of histone proteins to form nucleosomes. Amino-terminal tails of core histones protrude from the nucleosome and are subject to a plethora of posttranslational modifications (PTMs), which regulate almost all cellular processes requiring access to DNA, in particular gene transcription (Zentner and Henikoff, 2013). Recent studies show that histone PTMs could act combinatorially, influencing each other in a context-dependent manner, writing a pseudo-"histone crosstalk" language (Lee et al., 2010).

Histone lysine methylation is a marker of both transcriptionally active and inactive chromatin, depending on the residue that is methylated, its degree of methylation (mono-, di-, or trimethylation; me1, me2, me3), and its position within the gene and in the genome. Methylation of histone H3 lysine 4 (H3K4) and H3K36 is generally associated with transcriptionally active genes, whereas methylation of H3K27 and H3K9 are generally hallmarks of condensed chromatin at silent loci (Greer and Shi, 2012).

H3K27 methylation is achieved by the lysine methyltransferase (KMT) Ezh2 within the Polycomb Repressive Complex 2 (PRC2) and H3K9 methylation by different H3K9-specific KMTs. Beyond their common functions in gene silencing, components of the H3K9 and H3K27 methylation machineries have been separately demonstrated to have similar roles in the control of many cellular processes, ranging from embryonic stem cell (ESCs) pluripotency (Dodge et al., 2004; Pereira et al., 2010a; Yuan et al., 2009) to cell differentiation (Ait-Si-Ali et al., 2004; Chen et al., 2012; Ezhkova et al., 2009; Palacios et al., 2010; Pasini et al., 2007) and cell reprogramming (Chen et al., 2013; Epsztejn-Litman et al., 2008; Pereira et al., 2010a). They have also been suggested to possibly target common genes in ESCs (Bilodeau et al., 2009; Yuan et al., 2009).

PRC2-mediated silencing of developmental genes is a general mechanism required for the pluripotent cells to correctly enter differentiation (Boyer et al., 2006; Lee et al., 2006). Likewise, in some adult stem and progenitor cells, PRC2 mediates gene silencing by ensuring the proper temporal expression of differentiation genes (Margueron and Reinberg, 2011).

The core PRC2 complex is composed of four proteins, Suz12, Eed, RbAp46/48, and Ezh2 (KMT6), the latter being the catalytic subunit that establishes di- and trimethylation of monomethylated H3K27. All the PRC2 core members are required for Ezh2 to exert its activity. However, several substoichiometric components, such as Jarid2, HDAC1/2, Aebp2, Phf1, MTF2, and Phf19, have been shown to interact with PRC2, suggesting the existence of significant interactions between Polycomb proteins and other chromatin regulators outside the strict definition of the Polycomb group. Although these "accessories" proteins seem not essential for PRC2 KMT activity, they appear to fine-tune PRC2 activity and to modulate its recruitment (Simon and Kingston, 2013).

In mammals, the mechanisms that govern the genomic targeting of PRC2 and the establishment of H3K27me3 remain poorly understood. Intriguingly, H3K27 monomethylation levels remain unaffected after PRC2 disruption in vivo (Schoeftner et al., 2006), suggesting the existence of a H3K27 monomethyltransferase other than a known PRC2 component. Although Ezh1, the Ezh2 homolog, has been suggested to play such a role (Shen et al., 2008), its activity toward H3K27 is controversial (Margueron et al., 2008).

Notably, the H3K9 KMT G9a (KMT1C) has been shown to methylate H3K27 in vitro and in vivo (Patnaik et al., 2004; Tachibana et al., 2001; Wu et al., 2011). G9a and G9a-Like Protein (GLP or KMT1D) are two well-known H3K9 KMTs primarily responsible for mono- and dimethylation of H3K9. They exist predominantly as a G9a–GLP heteromeric complex, which appears to be a functional H3K9 methyltransferase in vivo (Tachibana et al., 2005).

Despite the aforementioned evidences in favor of a crosstalk between H3K9 and H3K27 methylations, a direct proof of a functional interplay between PRC2 and H3K9 KMTs in vivo is still lacking. Our results demonstrate that PRC2 interacts physically and functionally with G9a and GLP. Genome-wide chromatin immunoprecipitation (ChIP-seq) and transcriptomic analyses show that PRC2 and G9a/GLP share a significant number of genomic targets and regulate expression of a subset of developmental and neuronal genes. This regulation is dependent on G9a enzymatic activity that mediates PRC2 recruitment.

Together, our data clearly suggest a functional cooperation between PRC2 and G9a/GLP to ensure epigenetic gene silencing at certain chromatin regions. This demonstrates a crosstalk between these two major epigenetic silencing machineries.

RESULTS

PRC2 Core Members Interact with the Main H3K9 KMTs in Cells

To investigate H3K9 KMTs and PRC2 cooperation, we first designed experiments to study their possible interactions. To this end, we carried out HA-Flag double-affinity immunopurification, as previously described (Fritsch et al., 2010), from either nuclear soluble (Figure 1A) or nucleosome-enriched (Figures S1A and S1C available online) protein fractions of HeLa cells stably expressing one of the main H3K9 KMTs: G9a, GLP, SETDB1, and Suv39h1. Western blot (WB) analyses showed that PRC2 core members copurified preferentially with G9a and GLP (Figures 1A and S1A) and at a very low extent with SETDB1 and Suv39h1 (Figures 1A and S1A; data not shown). Hence, we decided to focus our further analysis on G9a and GLP.

To confirm the interaction between PRC2 core members and G9a/GLP, we performed endogenous coimmunoprecipitation (coIP) assays in mESCs and demonstrated that Ezh2 and Eed coprecipitated G9a and GLP (Figure 1B; data not shown). Conversely, Ezh2, Suz12, and Eed coprecipitated with G9a and GLP (Figure 1B). Notably, Jarid2 was found to interact with PRC2 core members (Figure 1B), as previously demonstrated (Li et al., 2010; Peng et al., 2009), and, in agreement with a previous report (Shirato et al., 2009), with G9a and GLP (Figure 1B and Figure S1C, right). However, since Jarid2 is a stable partner of PRC2, we cannot exclude the possibility that G9a/GLP-Jarid2 interactions could be mediated by PRC2. As a negative control, we tested YY1 interaction, and we detected it after neither PRC2 nor H3K9 KMTs IPs (Figure 1B).

Collectively, these results indicate that PRC2 and H3K9 KMTs physically interact both in human HeLa cells and mESCs. We obtained similar results in mouse myoblasts (data not shown), suggesting that these interactions are conserved in different species and tissues.

H3K9 KMTs Interact with PRC2 Core Members In Vitro

We next sought to test for direct interactions between PRC2 core members and G9a/GLP in vitro. We purified a recombinant PRC2 complex (Margueron et al., 2008) (Figure 1C), performed a pull-down with GST-G9a/GLP at different stringencies, and confirmed a strong interaction between PRC2 and G9a/GLP (Figure 1D). To further explore which PRC2 subunit could interact directly with G9a and GLP, we purified two PRC2 subcomplexes containing either Ezh2-Eed or Ezh2-Suz12-RbAp48 (Figure 1E) and performed pull-down assays with GST-G9a/GLP. We showed that both PRC2 subcomplexes strongly interact with G9a and GLP (Figures 1F and 1G), likely suggesting that interactions occur through the Ezh2 subunit. In an attempt to define the domain of G9a responsible for interaction with PRC2, we used in vitro-translated deletion mutants of G9a. While the full-length G9a, as well as the SET and the ankyrin-repeats deletion mutants, interacted with PRC2, the N-terminal deletion mutant did not show any interaction (Figure S1B). These results suggest that PRC2 interacts with G9a via its N-terminal domain.

We next tested whether G9a/GLP-PRC2 interaction was dependent on DNA or RNA. Our results showed that immunoprecipitation of either G9a or GLP from chromatin fractions treated with benzonase, known to digest both DNA and RNA, still coprecipitated PRC2 core subunits along with Jarid2, although at a lesser extent (Figure S1C). This could be explained by the fact that benzonase treatment induced a certain decrease in G9a/GLP protein levels (Figure S1C, input).

Altogether, these data show that PRC2 interacts directly with G9a/GLP, most likely via Ezh2 subunit, in absence of nucleic acids.

G9a/GLP and PRC2 Regulate Common Genes Encoding Developmental Regulators

We reasoned that if G9a/GLP cooperate functionally with PRC2, they should regulate a common set of target genes. Thus, we measured PRC2 target genes expression in wild-type (WT) and in *G9a*$^{-/-}$, *GLP*$^{-/-}$, or *G9a*$^{-/-}$/*GLP*$^{-/-}$ (hereafter referred as dKO) mESCs (Tachibana et al., 2008; Tachibana et al., 2005). Notably, expression of PRC2 core members is not affected by the absence of G9a and/or GLP (Figure S2A).

Interestingly, we found that a set of developmental regulators previously described to be direct targets of PRC2 (Boyer et al., 2006; Lee et al., 2006), which we confirmed using *Eed*$^{-/-}$ cells (Figure S2B), were also derepressed in mESCs lacking *G9a* and/or *GLP* or both, while pluripotency markers, such as *Oct4*, remain unaffected (Figure 2A). We did not notice any synergistic effect in *G9a*/*GLP* dKO cells (Figure 2A). However, other known

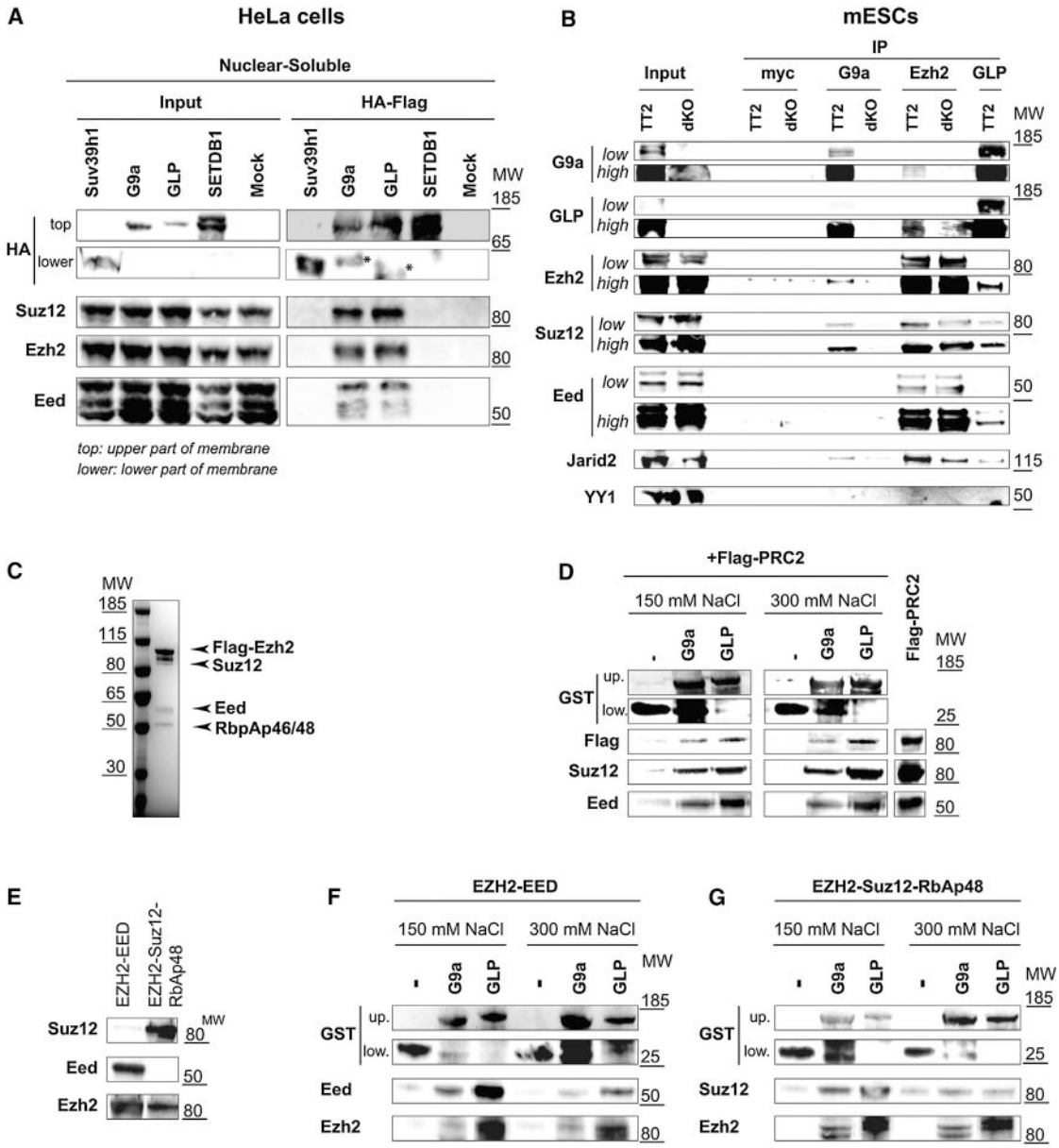

Figure 1. PRC2 Core Members Preferentially Interact with G9a/GLP H3K9 KMTs

(A) Endogenous PRC2 subunits coprecipitate with ectopically expressed G9a and GLP. HA-Flag-tagged Suv39h1, G9a, GLP, and SETDB1 complexes were purified from nuclear soluble fraction of HeLa cells as described in Fritsch et al. (2010) and subjected to western blot (WB) analyses with the indicated antibodies (Abs). Note that to detect Suv39h1 in the input we had to load ten times more material than G9a, GLP, and SETDB1. Asterisks indicate signal due to degradation or aborted translation of HA-G9a and HA-GLP.

(B) PRC2 members and G9a/GLP interact endogenously in mESCs. Nuclear extracts from WT (TT2) and *G9a*$^{-/-}$/*GLP*$^{-/-}$ (dKO) mESCs were used for immunoprecipitation (IP) with the indicated Abs; myc Ab was used as negative control. The resulting precipitates were then subjected to WB with indicated Abs. For some WBs, lower (low) and higher (high) exposures are shown.

(C) Simply Blue staining of a Flag-tagged purified PRC2 complex, from nuclear extracts of SF9 cells infected with baculoviruses expressing Flag-Ezh2, Suz12, Eed, and RbpAp48.

(D) G9a and GLP interact with PRC2 in vitro. Equivalent amounts of GST-G9a or GST-GLP were incubated with the Flag-PRC2 complex shown in (C). (–), GST-mock negative control. Interactions were tested at 150 or 300 mM NaCl and revealed by WB with the indicated Abs. up. and low., upper and lower part of membrane.

(E–G) G9a and GLP interact with PRC2 in vitro, likely through Ezh2 subunit. (E) WB on inputs for PRC2 subcomplexes used in (F) and (G). Ezh2-Eed and Ezh2-Suz12-RbpAp48 complexes were purified from SF9 cells. Equivalent amounts of GST-G9a or GST-GLP were incubated with the PRC2 subcomplexes Ezh2-Eed (F) or Ezh2-Suz12-RbpAp48 (G). (–), GST-mock negative control. Interactions were tested at 150 or 300 mM NaCl and revealed by WB with the indicated Abs. up./low., upper and lower part of membrane. MW, molecular weight marker in KDa.

See also Figure S1.

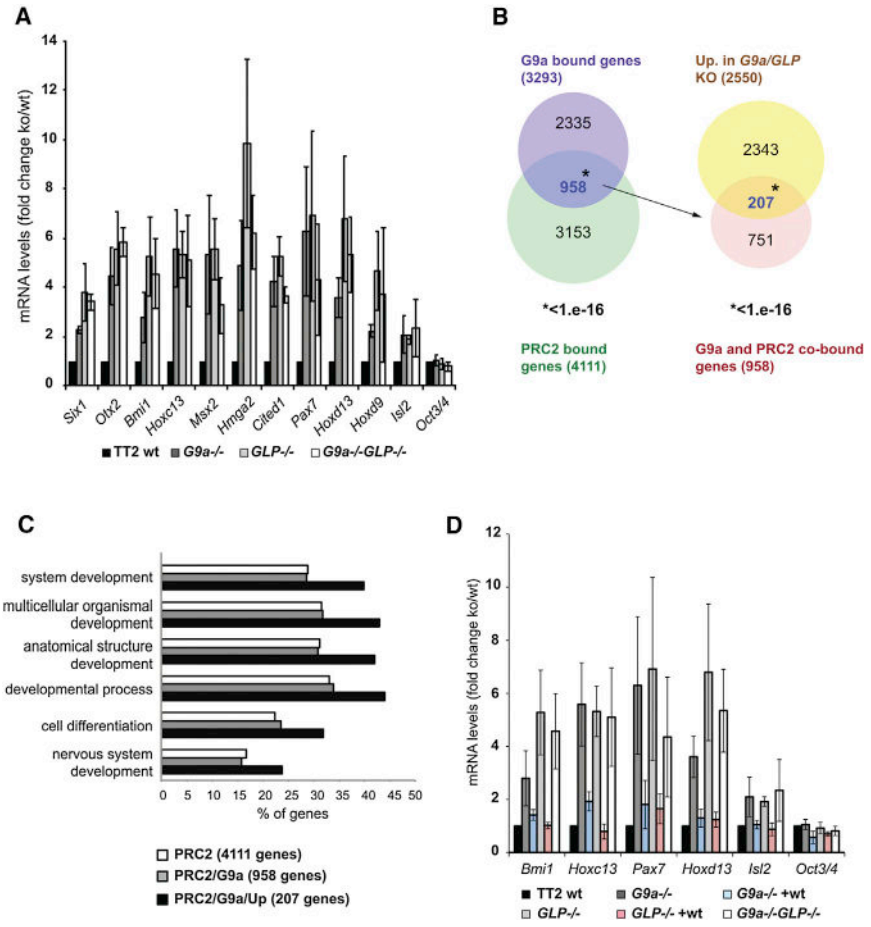

Figure 2. G9a/GLP and PRC2 Regulate Common Genes Encoding Developmental Regulators

(A) A group of PRC2 target genes are derepressed in the absence of G9a and/or GLP. qRT-PCR expression analysis in pluripotent WT (TT2), *G9a*$^{-/-}$, *GLP*$^{-/-}$, and *G9a*$^{-/-}$/*GLP*$^{-/-}$ mESCs shows derepression of the indicated PRC2 target genes. Data are represented as fold change (KO over WT) and as mean ± SEM, n ≥ 3.

(B) G9a/GLP and PRC2 regulate common genes. (Left) Venn diagram showing overlap between G9a-bound and PRC2 target genes. A statistically significant number of genes (958; *p < 10^{-16} according to hypergeometric test) were cobound by G9a and PRC2. (Right) Venn diagram showing that a significant number of the 958 G9a/PRC2 cobound genes (207; *p < 10^{-16} according to hypergeometric test) were upregulated (fold change ≥1.2; p < 0.05) in the absence of *G9a* and/or *GLP*. Note that with a hypergeometric test the expected number of a random overlap crossing 958 (PRC2/G9a-bound genes) with 2,550 terms (upregulated genes in absence of G9a/GLP) would be between 90 and 130. PRC2-bound genes were defined as enriched regions ±10 kb from transcription start site (TSS) by intersection of two different data sets: Suz12 ChIP-seq (Peng et al., 2009) and our Ezh2 ChIP-seq in TT2 mESCs (p < 10^{-3}) (Figure S2D). G9a-bound genes were defined as enriched regions (p < 10^{-2}) ±10 kb from TSS by the intersection of ChIP-seq biological duplicate: ChIP-seq of endogenous G9a in TT2 and of ectopically expressed G9a-wt in *G9a*$^{-/-}$ mESCs.

(C) G9a/GLP and PRC2 coregulate a subset of developmental regulators. GO analysis has been performed on PRC2 target genes (as defined in Figure S2E), PRC2/G9a target genes (defined in Figure 2B, left), and PRC2/G9a target genes upregulated in *G9a/GLP* KO (defined in Figure 2B, right). The graph shows top GO categories for biological processes.

(D) G9a and GLP re-expression in *G9a*$^{-/-}$ or *GLP*$^{-/-}$ mESCs restores PRC2 target genes repression. qRT-PCR expression analyses in mESCs described in (A) and in *G9a*$^{-/-}$ and *GLP*$^{-/-}$ mESCs rescued with either wt-G9a or wt-GLP. Data are represented as fold change (KO over WT) and as mean ±SEM, n ≥ 3.

See also Figure S2 and Table S1.

PRC2 targets seemed either unaffected or slightly derepressed in the absence of G9a or GLP (Figure S3B).

This prompted us to compare mRNA expression profiles at the global level in WT, *G9a*$^{-/-}$, *GLP*$^{-/-}$, and dKO mESCs. Correlation plots for the three different microarray data sets showed a strong correlation (r > 0.62 in all cases and p < $1e^{-16}$) between the fold change of expression in *G9a*$^{-/-}$, *GLP*$^{-/-}$, and dKO compared to WT mESCs (Figure S2C). Of note, some genes that were not detected as upregulated in all three cell lines by microarray analyses were in fact detected by qPCR (data not shown). Thus, we decided to consider the union of the genes differentially regulated in the three different KOs as genes generally deregulated (either up- or downregulated) in the absence of G9a/GLP.

By crossing our microarray results with published data generated from *Ezh2*$^{-/-}$ and *Eed*$^{-/-}$ mESCs (Shen et al., 2008), we found that 487 genes were commonly upregulated both in the absence of G9a/GLP or Ezh2/Eed and involved in cell differentiation and embryonic development (Figure S2D). We probably underestimated the number of coregulated genes, since we were not able, for example, to detect *pax7* (Figure 2A) upregulated in *G9a/GLP* KO cells in our microarray analysis. Moreover, by performing the same type of analysis with downregulated genes, we found a significant overlap of commonly downregulated genes, which were neither enriched in a specific biologically relevant Gene Ontology (GO) category nor preferentially cobound by G9a/PRC2 (data not shown). This observation suggests that G9a/PRC2 preferentially cotarget silenced genes.

To definitely unravel commonly regulated genes by G9a/GLP and PRC2, we coupled expression analysis to G9a and PRC2 genome-wide localization. To this end, we performed G9a and Ezh2 ChIP-seq in mESCs and analyzed the extent of their overlap, combined to the use of published Suz12 ChIP-seq (Boyer et al., 2006; Peng et al., 2009) (Figure S2E). We found 958 genes to be cobound by G9a and PRC2 (Figure 2B, left; Table S1), out of which a statistically significant number (207) was upregulated in the absence of *G9a* and/or *GLP* (Figure 2B, right; Table S1). Notably, we found the same proportion of genes to be both

cobound by G9a/PRC2 and upregulated in each of the three KO cell lines (data not shown). Interestingly, GO analysis showed significant enrichment in genes involved in development and differentiation, strikingly resembling classical GO of PRC2 targets (Figure 2C). The overlap with downregulated genes in *G9a/GLP* KO cells was instead not significant (Figure S2F), confirming that PRC2 and G9a preferentially cobind repressed genes. Indeed, by crossing common upregulated genes in absence of both G9a/GLP and PRC2 (Figure S2D) with PRC2/G9a cobound genes (Figure 2B), we still found a significant overlap (Figure S2G).

To further confirm our results, we also performed RNA-seq in WT versus $G9a^{-/-}$ mESCs cells. Among a total of 2567 upregulated genes in $G9a^{-/-}$ mESCs, a statistically significant number (175) was upregulated and cobound by G9a and PRC2 (Figure S2H, left panel). Moreover, considering only the genes found upregulated by both RNA-seq and microarray in $G9a^{-/-}$ mESCs, we still found a significant number cobound by PRC2-G9a (Figure S2H, right panel).

Thus, using different complementary approaches and cross-correlation methods, we constantly found a significant number of common upregulated and cobound genes, clearly demonstrating that G9a/GLP and PRC2 coregulate a subset of common target genes.

To definitely demonstrate that derepression of PRC2 target genes was due to the absence of G9a/GLP, we then measured the expression of these genes in $G9a^{-/-}$ and $GLP^{-/-}$ mESCs respectively rescued with wt-G9a or wt-GLP (Tachibana et al., 2008). In fact, G9a and GLP rescue did not affect PRC2 core members expression (Figure S2A) but was able to re-establish PRC2 target genes repression in mESCs (Figure 2D, blue and red bars).

Altogether, the evidences collected so far clearly suggest that G9a/GLP could cooperate directly with PRC2 to regulate a subset of genes encoding developmental regulators.

G9a/GLP Control PRC2 Recruitment and H3K27 Trimethylation at Genomic Loci

We next sought to investigate a possible interplay between G9a/GLP and PRC2 at the chromatin level. Thus, we analyzed PRC2 occupancy at its target genes in mESCs lacking G9a/GLP. ChIP-qPCR assays showed an impairment of Ezh2 recruitment at many of its known target *loci* (Figure 3A, left) in the absence of G9a and/or GLP, accompanied by a slight decrease in H3K27me3 (Figure 3A, middle). To confirm these findings on a global scale, we performed Ezh2 ChIP-seq and found a global reduction of Ezh2 occupancy in $G9a^{-/-}/GLP^{-/-}$ cells as compared to WT mESCs (Figure 3B). This effect is not due to a global delocalization of PRC2 from chromatin in the absence of G9a/GLP, as confirmed by nuclear fractionation (Figure 3C). Indeed, we found Ezh2 reduction to be specific of discrete loci (i.e., *Six1* and *Hmga2*) (Figure 3D), as compared to other Ezh2-bound genes, which did not show any G9a/GLP-dependent binding (i.e., *cd83*, *Osr1*; Figure S3A, upper panel). Interestingly, some genes which are not derepressed (i.e., *Onecut1*, *Gata4*; Figure S3B) show loss of Ezh2 binding in *G9a/GLP* KO cells (Figure S3A, lower panel), thus suggesting that loss of Ezh2 is not a consequence of derepression but rather a direct effect of G9a/GLP absence. In fact, by comparing peak-by-peak Ezh2 enrichment relative to the total amount of reads, we found that loss of Ezh2 occupancy was significantly higher for G9a/Ezh2 cobound genes than for Ezh2-only bound genes in the absence of *G9a/GLP* (Figure S3C). We also detected Ezh2 loss of binding on other G9a unbound genes, which could be due to derepression of indirect targets (468 genes) and/or to a more global effect of G9a loss (see the Discussion).

Altogether, these results clearly suggest that G9a/GLP could control PRC2 recruitment and H3K27 methylation at a significant subset of its target genes in mESCs.

G9a Controls Ezh2 Recruitment and H3K27 Trimethylation on an Artificial Promoter

To further confirm the G9a-dependent recruitment of Ezh2, we used the heterologous reporter T-REx system in which HEK293 T-REx cells contain a stably integrated luciferase (*Luc*) reporter gene expressed under the control of the thymidine kinase (TK) basal promoter with five GAL4 UAS (Li et al., 2010).

We generated a HEK293 T-REx cell line stably expressing a GAL4-G9a (WT or catalytic mutant) fusion protein or GAL4-PR-Set7 (negative control) under a doxycycline (doxy)-regulated promoter (Figure 4A). Doxycycline addition induced expression of GAL4-fused proteins (Figure 4B). ChIP using anti-GAL4 antibody demonstrated an efficient recruitment of GAL4- wt or mutant G9a and PR-Set7 at *luciferase* TSS after doxycycline induction (Figure 4C). G9a WT, but not the G9a catalytic mutant recruitment, resulted in increased levels of H3K9me2 (Figure 4D). Interestingly, WT G9a, but not G9a catalytic mutant or PR-Set7, led to the concomitant recruitment of Ezh2 (Figure 4E) and increased H3K27me3 (Figure 4F), suggesting requirement of G9a enzymatic activity in PRC2 recruitment and H3K27me3 establishment. In addition, WT G9a and G9a catalytic mutant, but not PR-Set7, repressed luciferase activity (Figure S4A). Finally, the use of the Ezh2-specific inhibitor GSK343 (Figure S4A) or siRNA-mediated Ezh2 downregulation (Figure S4D) modestly prevented G9a-induced luciferase repression (Figures S4A and S4E) and increase of H3K27me3 at *Luc* TSS (Figure S4F). Notably, GSK343 did not impair H3K9me2 global level in cells (Figure S4B), nor G9a enzymatic activity in vitro (Figure S4C). Together, these data suggest a possible cooperation between the two enzymatic activities.

To further assess the role of G9a in H3K27me3 establishment, we performed an in vitro methylation assay using reconstituted nucleosomes with recombinant histones, free of PTMs. We show that WT G9a, but not a G9a catalytic mutant, is able to monomethylate H3K27, further enhancing PRC2 trimethylation of this lysine (Figures S4G and S4H).

Collectively, these data indicate that G9a can regulate PRC2 recruitment to a genomic region to establish gene silencing, suggesting an involvement of G9a-mediated methylation in PRC2 genomic targeting and activity.

Ezh2 Recruitment Is Dependent on G9a Enzymatic Activity

To further confirm that PRC2 recruitment was dependent on G9a, we performed Ezh2 ChIP analysis in $G9a^{-/-}$ mESCs rescued with WT G9a. Moreover, in an attempt to test if G9a

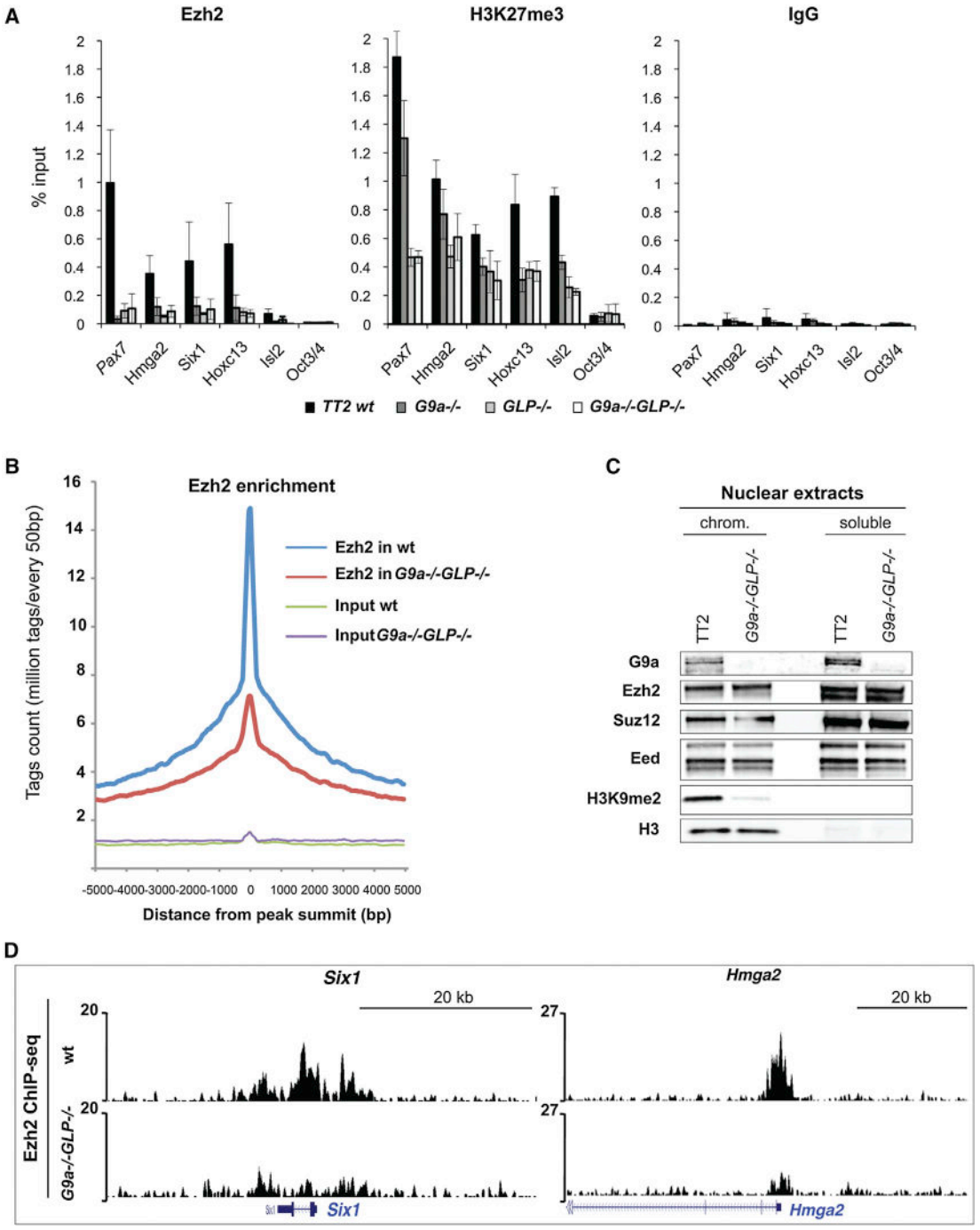

Figure 3. G9a/GLP Control PRC2 Occupancy at Target Genes

(A) Ezh2 and H3K27me3 target occupancy is impaired in the absence of G9a and/or GLP. ChIP q-PCR analyses of Ezh2 (left panel) and H3K27me3 (middle panel) in WT (TT2), *G9a*$^{-/-}$, *GLP*$^{-/-}$, and *G9a*$^{-/-}$/*GLP*$^{-/-}$ mESCs. The immunoprecipitated material was quantified by qPCR, and results are expressed as a percentage of immunoprecipitated DNA compared to the input DNA (% input). IgG (right panel) has been used as negative control. Data are represented as mean ±SEM, n ≥ 3.

(B) Global reduction of Ezh2 occupancy in *G9a*$^{-/-}$/*GLP*$^{-/-}$ mESCs. Ezh2 genome-wide recruitment has been analyzed by ChIP-seq in WT versus *G9a*$^{-/-}$/*GLP*$^{-/-}$ mESCs. Graph represents average binding density of genomic regions surrounding (±5 kb) Ezh2 binding sites (p value 5 × 10^{-5}) in mESCs; Ezh2 occupancy and inputs density in WT and *G9a*$^{-/-}$/*GLP*$^{-/-}$ mESCs are plotted as the average of reads density (every 50 bp) normalized to the total number of reads.

(C) PRC2 core member subnuclear localization is not affected in *G9a*$^{-/-}$/*GLP*$^{-/-}$ mESCs. Soluble and chromatin-enriched (chrom) nuclear fractions were isolated from WT TT2 and *G9a*$^{-/-}$/*GLP*$^{-/-}$ mESCs and analyzed by WB with the indicated antibodies.

(D) Genome browser representations of Ezh2 binding patterns in WT and *G9a*$^{-/-}$/*GLP*$^{-/-}$ mESCs at known PRC2 target loci.

See also Figure S3 and Table S1.

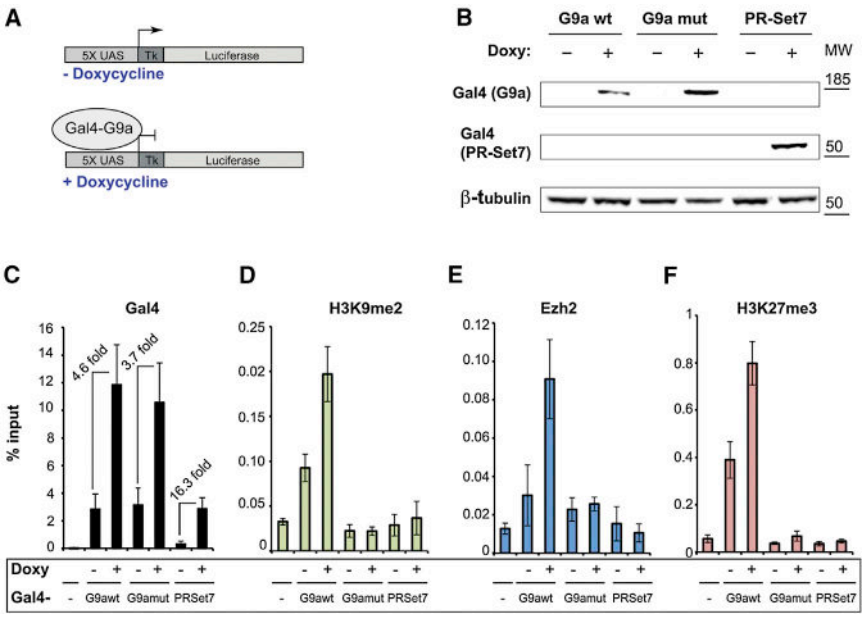

Figure 4. G9a-Dependent H3K9 Methylation Drives Ezh2 Binding and H3K27me3 Establishment on an Artificial Promoter

(A) Schematic representation of 5X GAL4-UAS-TK-Luc reporter system, stably integrated in HEK293 cells (T-REx system). Cells were stably transfected with either GAL4-G9a (WT or catalytic mutant) or GAL4-PR-SET7, as a negative control, and grown in the presence (+) or absence (–) of doxycycline for 24 hr.

(B) WB analysis to check expression of GAL4 fusion proteins upon doxycycline induction. β-tubulin, loading control.

(C–F) G9a recruitment to *Luc* promoter leads to PRC2 and H3K27me3 targeting. T-REx cells stably expressing G9a-wt, G9a catalytic mutant, or PR-SET7 fused to the GAL4 DNA-binding domain (GAL4-G9a wt, GAL4-G9a mut, or GAL4-PR-SET7) were grown in the presence (+) or absence (–) of doxycycline (doxy) for 24 hr. ChIP experiments for Gal4 (A), H3K9me2 (B), Ezh2 (E), and H3K27me3 (F) were performed, and DNA enrichment was analyzed at the TSS of *Luciferase* transgene. (C) Fold induction between +doxy versus – doxy calculated as the ratio of percent input in +doxy/–doxy. Data are represented as percent of input and as mean ±SEM, n = 3.

See also Figure S4.

enzymatic activity was crucial for PRC2 recruitment, we took advantage of previously established *G9a*$^{-/-}$ mESCs rescued with full-length enzymatic-inactive G9a. We used, in particular, the C1668A G9a mutant that is still able to heterodimerize with GLP. Rescued G9a (WT and mut) was slightly overexpressed in *G9a*$^{-/-}$ compared to WT mESCs (Figure 5A; Tachibana et al., 2008). H3K9me2 was only re-established by re-expression of WT G9a, and not by G9a catalytic mutant, at PRC2 target loci (Figure 5B). Strikingly, we found that only rescue with WT G9a, but not with G9a mutant, was able to re-establish Ezh2 occupancy and H3K27me3 at PRC2 target genes (Figure 5C).

Next, we checked if G9a protein per se was actually recruited at the same genomic loci. Our ChIP experiments showed that G9a was effectively found at PRC2 target genes in WT, as compared to *G9a*$^{-/-}$ mESCs (Figure 5D; black versus white bars). Moreover, G9a recruitment was higher in *G9a*$^{-/-}$ mESCs rescued with WT G9a (dark gray bars, Figure 5D), likely because of its increased re-expression (Figures 5A and S2A). Interestingly, this overexpression of G9a induced more Ezh2 recruitment and H3K27me3 at tested loci (Figure 5C). Notably, G9a catalytic mutant was targeted to the chromatin at comparable levels than endogenous protein, even if at lesser extent compared to rescued G9a WT (Figure 5D). In accordance with our results with the T-Rex system (Figure 4), Ezh2, H3K27me3, and H3K9me2 levels were not re-established with G9a mutant (Figures 5B and 5C). Furthermore, re-expression of G9a catalytic mutants (C1168A and H1113K) failed to restore normal silencing of PRC2 target genes (Figure S5A, as compared to WT G9a in Figure 2D).

To confirm that G9a enzymatic activity is required in PRC2 target gene silencing, we used the G9a/GLP-specific inhibitor UNC0642, which induces global decrease in H3K9me2, but not in H3K27me3, levels (Figure S5B). In these conditions, our results clearly show that a subset of PRC2 target genes was derepressed and Ezh2 recruitment impaired (Figures S5C and S5D). Moreover, the observation that acute pharmacological inhibition of G9a/GLP activity in WT mESCs is sufficient to induce PRC2 target genes' deregulation and impairment in PRC2 recruitment, in addition to G9a/GLP rescue experiments in KO cells, clearly rules out any possibility that these effects might be indirect consequences of knockout cell lines variability. These data rather reinforce the idea that PRC2 recruitment and gene silencing to a subset of its targets is dependent on G9a/GLP enzymatic activity.

G9a and PRC2 Colocalize Genome-wide Preferentially at Promoters

Since the genome-wide distribution of G9a has never been studied so far, we wanted to finely analyze G9a preferential genomic binding elements and, lately, unravel the physiological pathways coregulated by G9a and PRC2.

We could observe that one-third of G9a target sites colocalize with known PRC2 members, notably Suz12 and Jarid2 (Figure 6A, lower panel), further supporting the notion that G9a and PRC2 can bind same genomic regions and regulate common target genes. We note that PRC2 binding sites (Suz12/Jarid2) cobound by G9a comprise sharp occupancy loci with sites enriched up to several kilobases, giving signals around ±5 kb. Using higher-stringency peak detection, we obtained similar proportion of G9a/PRC2 overlap (data not shown). Conversely, G9a recovered approximately 10% of PRC2 binding sites (data not shown).

Analyzing the distribution of G9a-binding sites relative to TSS, we could evidence that G9a is enriched around promoters

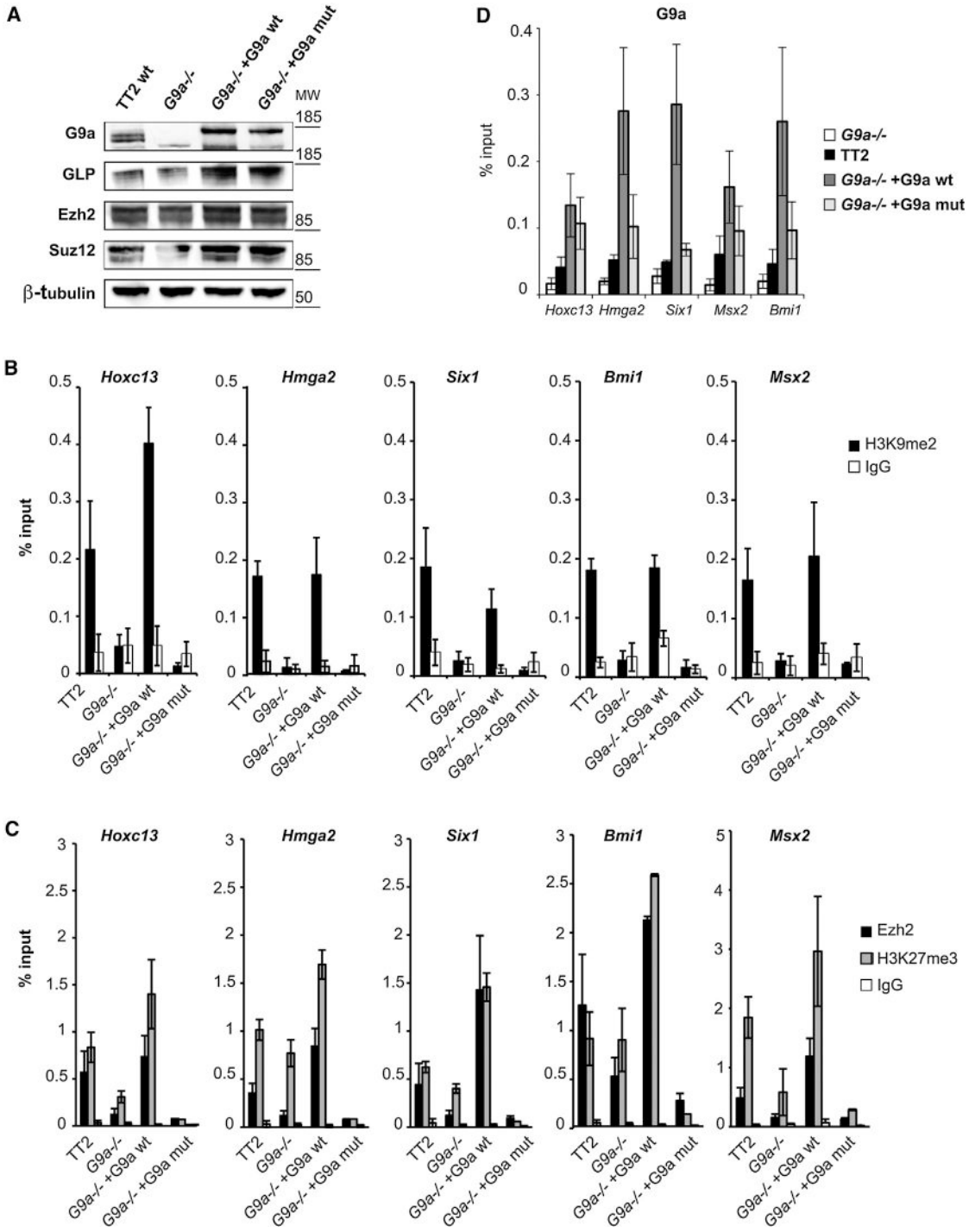

Figure 5. PRC2 Recruitment Is Dependent on G9a Enzymatic Activity

(A) PRC2 member expression is not affected in *G9a*$^{-/-}$ mESCs. WB analysis of total protein extracts from wild-type (TT2), *G9a*$^{-/-}$, *G9a*$^{-/-}$ rescued with a wild-type version of G9a (G9a-wt) and *G9a*$^{-/-}$ rescued with a G9a inactive mutant C1168A (G9a-mut) mESCs shows correct re-expression of G9a and no differences in protein levels of PRC2 core members. β-tubulin, loading control.

(B) H3K9me2 at PRC2 target loci. H3K9me2 binding at known PRC2 genomic targets has been analyzed by ChIP-qPCR in the same samples described in (A). IgG were used as ChIP negative control. Data are represented as percent of input and as mean +/− SEM, n = 3.

(C) Ezh2 and H3K27me3 target occupancy is rescued by G9a-wt, but not by G9a-inactive mutant. Ezh2 (black bars) and H3K27me3 (gray bars) binding at known PRC2 genomic targets have been analyzed by ChIP-qPCR in the same samples described in (A). IgG (white bars) was used as ChIP negative control. Data are represented as percent of input and as mean +/− SEM, n = 3.

(legend continued on next page)

(Figures 6B and S6A, upper). Accordingly, Polycomb proteins are known to be preferentially associated around promoters at CpG islands (Mendenhall et al., 2010). Indeed, we found G9a/Suz12 cobound sites to be enriched around promoters and CpG islands as compared to G9a alone (Figures 6B, S6B, and S6C). Interestingly, the G9a-binding sites, excluding G9a/Suz12 cobound sites, are instead enriched in LTRs (Figures S6B and S6C). In agreement with our observation, it has been reported that G9a binds LTRs, more specifically mouse endogenous retroviral elements or MERVs (Maksakova et al., 2013).

G9a and PRC2 Colocalize at Neuronal Genes

Interestingly, GO analysis of the G9a/PRC2 cobound genes mirrored categories associated with development (Figure 2C), as for Polycomb and G9a proteins (Figures 2C and S6D). In particular, pathways involved in neuronal differentiation were enriched (Figure 2C), compared to all G9a targeted categories (Figure S6D). This observation is in agreement with the well-known role of G9a as a regulator of the nervous system functions (Maze et al., 2010; Schaefer et al., 2009). Accordingly, we found genomic colocalization between G9a, PRC2, and the neuronal regulator REST (Figure 6A, lower), which has been shown to interact both with G9a and PRC2 (Dietrich et al., 2012; Roopra et al., 2004). Indeed, we found that G9a forms a ternary complex with REST and PRC2 (also with CDYL; data not shown), supporting the notion that such a complex might function to silence common target genes (Figure 6A, upper panel). Accordingly, we found genomic colocalization of G9a, Suz12, and REST on promoter regions of neuronal genes (Figure 6C). We confirmed by ChIP-qPCR the concomitant presence of G9a, Ezh2, H3K9me2, and H3K27me3 at the promoter regions of many key neural-specific genes in WT mESCs (Figure 6D). Notably, G9a enzymatic activity is required in PRC2 recruitment (Figure 5), while G9a binding is not impaired in *Eed*$^{-/-}$ cells (Figure S6E).

Together, these observations suggest a common role for G9a and PRC2 in the maintenance of neuronal genes silencing.

DISCUSSION

Histone H3 methylations on lysines 9 and 27 are among the major gene silencing mechanisms in eukaryotes, which function as guard keepers of facultative heterochromatin to maintain gene silencing. Recent genome-wide studies suggest that PRC2 and H3K9 KMTs might colocalize at some genomic regions (Bilodeau et al., 2009; Wang et al., 2008; Yuan et al., 2009). Nonetheless, a functional interdependence between H3K9 KMTs and PRC2 has thus far never been addressed. Here we asked whether the H3K9 and H3K27 methylations could be interdependent and cooperate to coregulate gene silencing.

The relative abundance of different epigenetic marks at precise lysine residues has recently emerged as a key strategy used by ESCs to fine-tune the expression of key genes involved in lineage commitment. Indeed, promoters of developmentally regulated genes that are repressed in pluripotent ESCs by H3K27me3 are also frequently marked by H3K4 methylation, which usually characterizes active chromatin. Through these *bivalent* domains, differentiation genes controlled by PRC2 are poised for activation upon removal of the repressive epigenetic marks (Bernstein et al., 2006; Mikkelsen et al., 2007; Pan et al., 2007). Recently, H3K9 methylation has also emerged as a further layer of regulation of pluripotency in stem cells (Alder et al., 2010). Indeed, it has been shown that H3K9me3 also marks bivalent genes in trophoblast stem cells, unraveling the existence of *trivalent* domains (H3K4me3/H3K27me3/H3K9me3) and suggesting that H3K9 and H3K27 methylations could act in synergy to stabilize a repressed state at silent genes. The finding that the H3K9 KMT SETDB1 colocalizes with PRC2 (Bilodeau et al., 2009; Yuan et al., 2009) suggested that these two machineries might cooperate to silence common target genes in ESCs. However, such cooperation has not been functionally addressed.

We have previously shown that a subset of H3K9 KMTs—Suv39h1, G9a, GLP, and SETDB1—form a complex and cooperate to progressively establish H3K9 trimethylation at specific loci (Fritsch et al., 2010). Here we show that PRC2 interacts with the mono- and dimethyltransferases G9a, GLP, and, to a much lesser extent, with the trimethyltransferases SETDB1 and Suv39h1. Of note, we noticed that G9a/GLP and PRC2 interact both in the chromatin-enriched and in the nuclear soluble fractions, yet this interaction is independent of nucleic acids. Interestingly, in vitro experiments showed that such interactions are direct and could involve the Ezh2 subunit, even under high salt concentrations, confirming in vivo data and that these proteins could interact in the absence of chromatin components (histones and DNA). In agreement with our findings, it has been observed that G9a/GLP and PRC2 coelute after size exclusion chromatography of mESC nuclear extracts (Chaturvedi et al., 2012).

ChIP-seq studies showed that di- and trimethylation of H3K9 and H3K27 seem to colocalize genome-wide in human cells (Wang et al., 2008). Accordingly, our genome-wide study clearly confirmed a significant overlap between G9a-bound genes and PRC2 targets. It is noteworthy that by performing ChIP-seq against H3K9 KMTs, we overcame the problem of possible crossreactivity between the antibodies raised against methylated H3K9 and H3K27 (Egelhofer et al., 2011). In particular, we found that G9a/PRC2 common target genes are mainly involved in development and neuronal differentiation, in line with many studies demonstrating a role for both G9a (Maze et al., 2010; Schaefer et al., 2009) and PRC2 (Dietrich et al., 2012; Pereira et al., 2010b) in the regulation of nervous system functions.

This finding was further supported by transcriptomic analyses performed in mESCs lacking *G9a* and/or *GLP*. We found a significant overlap between PRC2 targets and genes upregulated in absence of G9a/GLP. This confirmed that G9a/GLP could cooperate with PRC2 to regulate gene expression, especially at a subset of developmental genes involved in neuronal differentiation.

(D) G9a is recruited at PRC2 target genes, regardless of its enzymatic activity. G9a binding in the same cells shown in (A) was assessed by ChIP-qPCR. G9a binds the same genomic regions shown in (B) in WT cells as compared to *G9a*$^{-/-}$. G9a binding is restored after G9a-wt and also G9a mutant (G9a-mut) re-expression. (B–D) Data are shown as the percent of input and as mean ±SEM, n ≥ 3.
See also Figure S5.

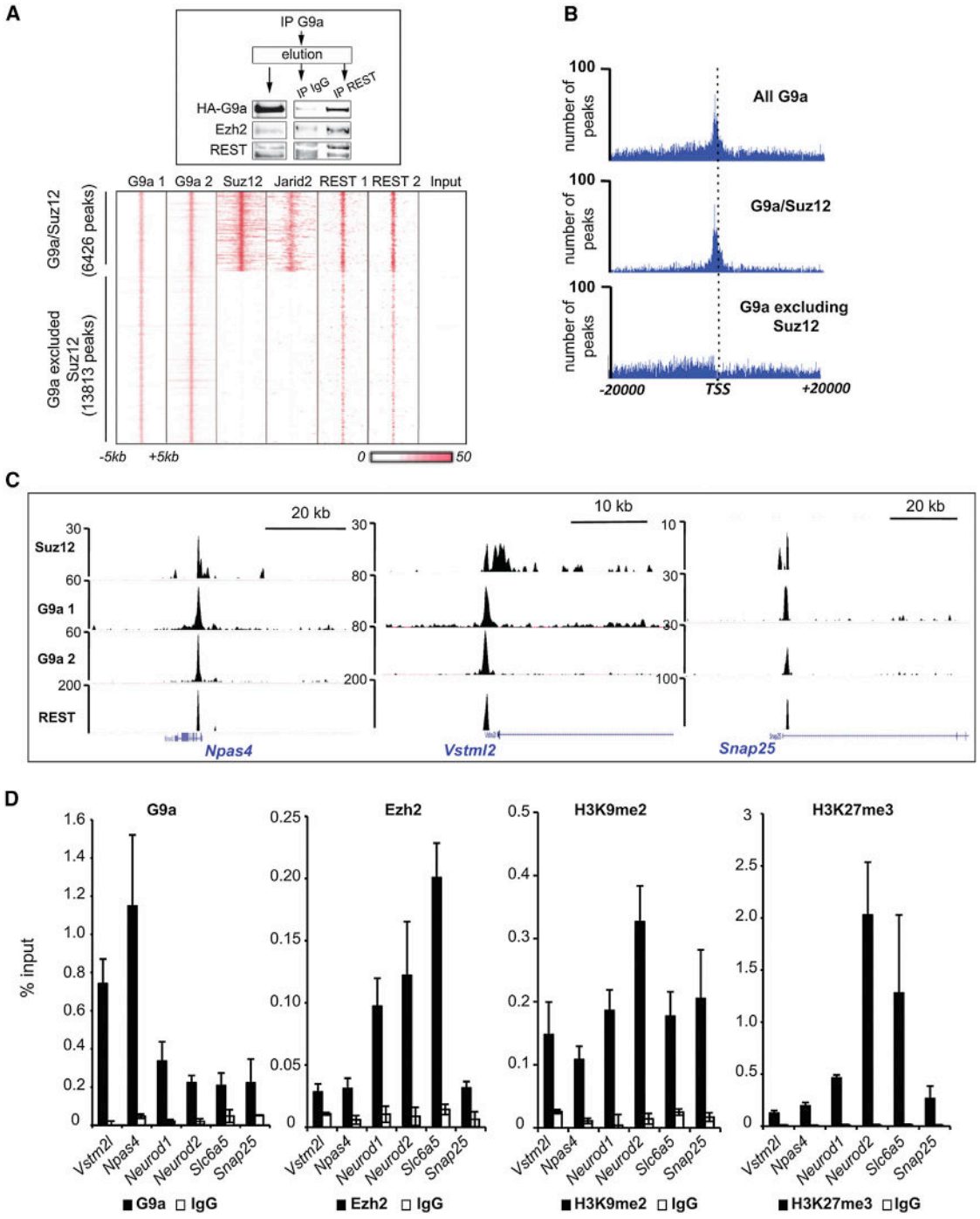

Figure 6. Genome-wide Colocalization of PRC2 and G9a

(A) (Upper panel) G9a forms ternary complex with REST and Ezh2. Tagged G9a was immunoprecipitated using anti-Flag Ab. Precipitated material was then subjected to a second IP step with either control IgG or anti-REST Ab. Resulting precipitates were analyzed with the indicated Abs. (Lower panel) Heatmaps showing binding regions (±5 kb) of endogenous G9a (G9a 1) and G9a-wt rescued in *G9a*$^{-/-}$ mESCs (G9a 2) which reveal overlap with Suz12 (Peng et al., 2009), Jarid2 (Li et al., 2010), and two different REST ChIP-seq (REST 1, Arnold et al., 2013; and REST 2, Whyte et al., 2012). Scale 0–50 of red color is proportional to read enrichment and normalized between ChIP-seq experiments for their total number of reads. Heatmap of input DNA is shown as a control.

(B) Peak distribution of G9a around TSS (±20 kb). Top panel represents all the 20,239 identified G9a peaks. Middle panel represents G9a and Suz12 overlapping binding sites (6,426). Bottom panel represents G9a without Suz12.

(legend continued on next page)

H3K9 and H3K27 lysines are embedded within a similar peptide sequence, namely ARKS, making plausible the existence of common modifying enzymes, such as the lysine demethylase KDM7 that demethylates both H3K9 and H3K27 (Tsukada et al., 2010). Interestingly, recent mass spectrometry studies have clearly shown that H3K27me2/3 nucleosomes purified from ESCs also harbor H3K9me2/3 (Voigt et al., 2012). This evidence strongly suggest that these two marks can be present on the same nucleosome(s) and thus on the same genomic regions. The H3K9 KMT G9a has been shown to methylate both H3K9 and H3K27 in vitro using recombinant histone H3 (Tachibana et al., 2001). Similarly, PRC2 demonstrated KMT activity in vitro toward H3K9 on histone tails and histone octamer (Kuzmichev et al., 2002). However, while H3K9 methylation levels are not affected in vivo in the absence of PRC2 (i.e., in *Eed*$^{-/-}$ mESCs) (Chamberlain et al., 2008), H3K27 monomethylation decreases significantly in the *G9a* and/or *GLP* KO cells (Wu et al., 2011). Indeed, our data showed that G9a monomethylates H3K27, which enhances subsequent PRC2-mediated trimethylation. This evidence suggests that G9a-mediated histone methylation increases PRC2 activity. Thus, it is tempting to speculate that in vivo G9a could monomethylate H3K27, which then serves as a substrate for subsequent PRC2 H3K27 di- and trimethylation. Since we have previously shown that Eed efficiently binds to H3K9-methylated nucleosomes (Margueron et al., 2009), it is possible that, at common genomic loci, G9a-mediated H3K9 and H3K27 monomethylation might serve as stimulating factors for subsequent PRC2 recruitment and activity.

Indeed, we showed here that Ezh2 recruitment and H3K27 trimethylation were impaired in *G9a* null mESCs. Interestingly, re-expression of WT, but not enzymatically inactive G9a, in *G9a*$^{-/-}$ mESCs restored Ezh2 recruitment, H3K27 trimethylation, and silencing of the deregulated PRC2-target genes. Loss of PRC2 at G9a/PRC2 cotargeted genes upon *G9a* depletion further indicates that PRC2 alone is not sufficient to ensure silencing and rather needs cooperation with G9a. These results strongly suggest that G9a and its methyltransferase activity are required in the maintenance of the PRC2-mediated gene silencing.

Intriguingly, G9a is able to methylate several nonhistone substrates, mainly epigenetic regulators (Rathert et al., 2008). It has also been shown that G9a automethylation mediates its interaction with epigenetic factors, such as HP1 or CDYL (Sampath et al., 2007), which also interact with REST and PRC2 (Mulligan et al., 2008; Zhang et al., 2011). Thus, another captivating speculation could be that G9a regulates PRC2 recruitment via its automethylation or methylation of a common targeting factor(s). Possible candidates might comprise Jarid2 and Snail1, which have been shown to interact with and mediate both PRC2 (Herranz et al., 2008; Pasini et al., 2010; Peng et al., 2009) and G9a/GLP (Dong et al., 2012; Shirato et al., 2009) targeting at some loci or REST, which has also been implied in genomic targeting of both G9a (Roopra et al., 2004) and PRC2 (Dietrich et al., 2012) and to bind enriched loci for H3K9me2 and H3K27me3 (Zheng et al., 2009). This hypothesis is in agreement with our data showing that G9a/PRC2 interact and colocalize genome-wide with REST and with the evidence that PRC2/G9a common targets are mainly involved in neuronal differentiation.

Moreover, the noncoding RNA *Kcnq1ot1* has been shown to bind both G9a and PRC2 (Pandey et al., 2008), suggesting that it could be implicated in G9a/PRC2 targeting. In fact, we have shown that benzonase treatment induces a certain level of G9a/GLP destabilization, suggesting that RNA could be involved in regulation of G9a/GLP stability or targeting.

In conclusion, our findings support a model through which G9a/GLP and PRC2 are corecruited to some genomic loci, likely via a common targeting factor. The evidence showing that PRC2 recruitment and activity are dependent on G9a-mediated methylation raises two possibilities, one involving G9a-mediated *cis*- or *trans*-methylation of this common targeting factor and the other implying histone methylation. These two hypotheses are not exclusive; we propose that G9a/GLP and PRC2 might be recruited via a common factor and that G9a-mediated H3K9 and/or H3K27 monomethylation might then stimulate PRC2 activity and/or recruitment at common genomic loci.

In the future, it would be interesting to study if such a functional interdependence between G9a and PRC2 occurs during neuronal lineage commitment. If this will be the case, it is intriguing to predict G9a/PRC2 pathway as a future pharmacological target in neuronal diseases.

EXPERIMENTAL PROCEDURES

Cell Culture

HeLa-S3, HEK293-T-Rex, and mESCs were cultured as detailed in the Supplemental Information.

Protein Complex Purification, CoIP

Double-affinity purification of Flag-HA-H3K9 KMTs, sequential IP, endogenous coIPs, and WB were carried as previously described (Fritsch et al., 2010) and detailed in the Supplemental Information.

GST Pull-Down

GST-recombinant proteins production and GST pull-down were performed as previously described (Fritsch et al., 2010). Flag-PRC2 recombinant complex was produced as described previously (Margueron et al., 2008).

RNA-seq, Microarray, and qRT-PCR

RNA-seq, microarray, and qRT-PCR are detailed in the Supplemental Information.

ChIP, ChIP-seq, and Bioinformatic Analyses

ChIP, ChIP-seq, and bioinformatic analyses are detailed in the Supplemental Information.

(C) Genome browser representation of genomic regions showing colocalization between G9a, Suz12, as in (A), and REST (Whyte et al., 2012) at three representative neuronal-specific genes and threshold from 3 to 4 up to 200 tag count every 10 pb window.
(D) ChIP-qPCR experiments in WT mESCs showing G9a, Ezh2, H3K9me2, and H3K27me3 enrichment at the promoter regions of neuronal-specific genes. Data are represented as percent of input and mean ±SEM, n ≥ 3.
See also Figure S6.

ACCESSION NUMBERS

ChIP-seq raw data are available at the Gene Expression Omnibus site under accession number GSE46545.

SUPPLEMENTAL INFORMATION

Supplemental Information includes six figures, one table, and Supplemental Experimental Procedures and can be found with this article at http://dx.doi.org/10.1016/j.molcel.2013.12.005.

ACKNOWLEDGMENTS

We warmly thank M. Ameyar-Zazoua, E. Boyarchuk, B. Miotto, C. Rougeulle, P.A. Defossez, S. Beyer, O. Ait-Mohamed, V. Battisti, V. Joliot, and J. Weitzman for critical reading of the manuscript. We thank Drs. Y. Shinkai, M. Tachibana, S. Orkin, M.R. Stallcup, D. Pasini, B.P. Zhou, M. Shapira, and SGC for generous sharing of reagents. We thank J.Y. Coppée, M.A. Dillies, F. Dumont, C. Vallot, and E. Nora for statistical/technical advice. This work was supported by the Agence Nationale de la Recherche (H3K9-methylome and EPILIS grants), the Association Française contre les Myopathies (AFM), the Fondation Bettencourt-Schueller, the Fondation ARC, GEFLUC, the Institut National du Cancer (INCa, grant 2012-1-PLBIO), CNRS, and Université Paris Diderot. C.M. was recipient of FRM and EMBO fellowships, and J.P. was recipient of PhD fellowships from the MESR and Fondation ARC.

Received: April 26, 2013
Revised: August 12, 2013
Accepted: November 26, 2013
Published: January 2, 2014

REFERENCES

Ait-Si-Ali, S., Guasconi, V., Fritsch, L., Yahi, H., Sekhri, R., Naguibneva, I., Robin, P., Cabon, F., Polesskaya, A., and Harel-Bellan, A. (2004). A Suv39h-dependent mechanism for silencing S-phase genes in differentiating but not in cycling cells. EMBO J. *23*, 605–615.

Alder, O., Lavial, F., Helness, A., Brookes, E., Pinho, S., Chandrashekran, A., Arnaud, P., Pombo, A., O'Neill, L., and Azuara, V. (2010). Ring1B and Suv39h1 delineate distinct chromatin states at bivalent genes during early mouse lineage commitment. Development *137*, 2483–2492.

Arnold, P., Schöler, A., Pachkov, M., Balwierz, P.J., Jørgensen, H., Stadler, M.B., van Nimwegen, E., and Schübeler, D. (2013). Modeling of epigenome dynamics identifies transcription factors that mediate Polycomb targeting. Genome Res. *23*, 60–73.

Bernstein, B.E., Mikkelsen, T.S., Xie, X., Kamal, M., Huebert, D.J., Cuff, J., Fry, B., Meissner, A., Wernig, M., Plath, K., et al. (2006). A bivalent chromatin structure marks key developmental genes in embryonic stem cells. Cell *125*, 315–326.

Bilodeau, S., Kagey, M.H., Frampton, G.M., Rahl, P.B., and Young, R.A. (2009). SetDB1 contributes to repression of genes encoding developmental regulators and maintenance of ES cell state. Genes Dev. *23*, 2484–2489.

Boyer, L.A., Plath, K., Zeitlinger, J., Brambrink, T., Medeiros, L.A., Lee, T.I., Levine, S.S., Wernig, M., Tajonar, A., Ray, M.K., et al. (2006). Polycomb complexes repress developmental regulators in murine embryonic stem cells. Nature *441*, 349–353.

Chamberlain, S.J., Yee, D., and Magnuson, T. (2008). Polycomb repressive complex 2 is dispensable for maintenance of embryonic stem cell pluripotency. Stem Cells *26*, 1496–1505.

Chaturvedi, C.P., Somasundaram, B., Singh, K., Carpenedo, R.L., Stanford, W.L., Dilworth, F.J., and Brand, M. (2012). Maintenance of gene silencing by the coordinate action of the H3K9 methyltransferase G9a/KMT1C and the H3K4 demethylase Jarid1a/KDM5A. Proc. Natl. Acad. Sci. USA *109*, 18845–18850.

Chen, X., Skutt-Kakaria, K., Davison, J., Ou, Y.L., Choi, E., Malik, P., Loeb, K., Wood, B., Georges, G., Torok-Storb, B., and Paddison, P.J. (2012). G9a/GLP-dependent histone H3K9me2 patterning during human hematopoietic stem cell lineage commitment. Genes Dev. *26*, 2499–2511.

Chen, J., Liu, H., Liu, J., Qi, J., Wei, B., Yang, J., Liang, H., Chen, Y., Chen, J., Wu, Y., et al. (2013). H3K9 methylation is a barrier during somatic cell reprogramming into iPSCs. Nat. Genet. *45*, 34–42.

Dietrich, N., Lerdrup, M., Landt, E., Agrawal-Singh, S., Bak, M., Tommerup, N., Rappsilber, J., Södersten, E., and Hansen, K. (2012). REST-mediated recruitment of polycomb repressor complexes in mammalian cells. PLoS Genet. *8*, e1002494.

Dodge, J.E., Kang, Y.K., Beppu, H., Lei, H., and Li, E. (2004). Histone H3-K9 methyltransferase ESET is essential for early development. Mol. Cell. Biol. *24*, 2478–2486.

Dong, C., Wu, Y., Yao, J., Wang, Y., Yu, Y., Rychahou, P.G., Evers, B.M., and Zhou, B.P. (2012). G9a interacts with Snail and is critical for Snail-mediated E-cadherin repression in human breast cancer. J. Clin. Invest. *122*, 1469–1486.

Egelhofer, T.A., Minoda, A., Klugman, S., Lee, K., Kolasinska-Zwierz, P., Alekseyenko, A.A., Cheung, M.S., Day, D.S., Gadel, S., Gorchakov, A.A., et al. (2011). An assessment of histone-modification antibody quality. Nat. Struct. Mol. Biol. *18*, 91–93.

Epsztejn-Litman, S., Feldman, N., Abu-Remaileh, M., Shufaro, Y., Gerson, A., Ueda, J., Deplus, R., Fuks, F., Shinkai, Y., Cedar, H., and Bergman, Y. (2008). De novo DNA methylation promoted by G9a prevents reprogramming of embryonically silenced genes. Nat. Struct. Mol. Biol. *15*, 1176–1183.

Ezhkova, E., Pasolli, H.A., Parker, J.S., Stokes, N., Su, I.H., Hannon, G., Tarakhovsky, A., and Fuchs, E. (2009). Ezh2 orchestrates gene expression for the stepwise differentiation of tissue-specific stem cells. Cell *136*, 1122–1135.

Fritsch, L., Robin, P., Mathieu, J.R., Souidi, M., Hinaux, H., Rougeulle, C., Harel-Bellan, A., Ameyar-Zazoua, M., and Ait-Si-Ali, S. (2010). A subset of the histone H3 lysine 9 methyltransferases Suv39h1, G9a, GLP, and SETDB1 participate in a multimeric complex. Mol. Cell *37*, 46–56.

Greer, E.L., and Shi, Y. (2012). Histone methylation: a dynamic mark in health, disease and inheritance. Nat. Rev. Genet. *13*, 343–357.

Herranz, N., Pasini, D., Díaz, V.M., Francí, C., Gutierrez, A., Dave, N., Escrivà, M., Hernandez-Muñoz, I., Di Croce, L., Helin, K., et al. (2008). Polycomb complex 2 is required for E-cadherin repression by the Snail1 transcription factor. Mol. Cell. Biol. *28*, 4772–4781.

Kuzmichev, A., Nishioka, K., Erdjument-Bromage, H., Tempst, P., and Reinberg, D. (2002). Histone methyltransferase activity associated with a human multiprotein complex containing the Enhancer of Zeste protein. Genes Dev. *16*, 2893–2905.

Lee, T.I., Jenner, R.G., Boyer, L.A., Guenther, M.G., Levine, S.S., Kumar, R.M., Chevalier, B., Johnstone, S.E., Cole, M.F., Isono, K., et al. (2006). Control of developmental regulators by Polycomb in human embryonic stem cells. Cell *125*, 301–313.

Lee, J.S., Smith, E., and Shilatifard, A. (2010). The language of histone crosstalk. Cell *142*, 682–685.

Li, G., Margueron, R., Ku, M., Chambon, P., Bernstein, B.E., and Reinberg, D. (2010). Jarid2 and PRC2, partners in regulating gene expression. Genes Dev. *24*, 368–380.

Maksakova, I.A., Thompson, P.J., Goyal, P., Jones, S.J., Singh, P.B., Karimi, M.M., and Lorincz, M.C. (2013). Distinct roles of KAP1, HP1 and G9a/GLP in silencing of the two-cell-specific retrotransposon MERVL in mouse ES cells. Epigenetics Chromatin *6*, 15.

Margueron, R., and Reinberg, D. (2011). The Polycomb complex PRC2 and its mark in life. Nature *469*, 343–349.

Margueron, R., Li, G., Sarma, K., Blais, A., Zavadil, J., Woodcock, C.L., Dynlacht, B.D., and Reinberg, D. (2008). Ezh1 and Ezh2 maintain repressive chromatin through different mechanisms. Mol. Cell *32*, 503–518.

Margueron, R., Justin, N., Ohno, K., Sharpe, M.L., Son, J., Drury, W.J., 3rd, Voigt, P., Martin, S.R., Taylor, W.R., De Marco, V., et al. (2009). Role of the

polycomb protein EED in the propagation of repressive histone marks. Nature *461*, 762–767.

Maze, I., Covington, H.E., 3rd, Dietz, D.M., LaPlant, Q., Renthal, W., Russo, S.J., Mechanic, M., Mouzon, E., Neve, R.L., Haggarty, S.J., et al. (2010). Essential role of the histone methyltransferase G9a in cocaine-induced plasticity. Science *327*, 213–216.

Mendenhall, E.M., Koche, R.P., Truong, T., Zhou, V.W., Issac, B., Chi, A.S., Ku, M., and Bernstein, B.E. (2010). GC-rich sequence elements recruit PRC2 in mammalian ES cells. PLoS Genet. *6*, e1001244.

Mikkelsen, T.S., Ku, M., Jaffe, D.B., Issac, B., Lieberman, E., Giannoukos, G., Alvarez, P., Brockman, W., Kim, T.K., Koche, R.P., et al. (2007). Genome-wide maps of chromatin state in pluripotent and lineage-committed cells. Nature *448*, 553–560.

Mulligan, P., Westbrook, T.F., Ottinger, M., Pavlova, N., Chang, B., Macia, E., Shi, Y.J., Barretina, J., Liu, J., Howley, P.M., et al. (2008). CDYL bridges REST and histone methyltransferases for gene repression and suppression of cellular transformation. Mol. Cell *32*, 718–726.

Palacios, D., Mozzetta, C., Consalvi, S., Caretti, G., Saccone, V., Proserpio, V., Marquez, V.E., Valente, S., Mai, A., Forcales, S.V., et al. (2010). TNF/p38α/polycomb signaling to Pax7 locus in satellite cells links inflammation to the epigenetic control of muscle regeneration. Cell Stem Cell *7*, 455–469.

Pan, G., Tian, S., Nie, J., Yang, C., Ruotti, V., Wei, H., Jonsdottir, G.A., Stewart, R., and Thomson, J.A. (2007). Whole-genome analysis of histone H3 lysine 4 and lysine 27 methylation in human embryonic stem cells. Cell Stem Cell *1*, 299–312.

Pandey, R.R., Mondal, T., Mohammad, F., Enroth, S., Redrup, L., Komorowski, J., Nagano, T., Mancini-Dinardo, D., and Kanduri, C. (2008). Kcnq1ot1 antisense noncoding RNA mediates lineage-specific transcriptional silencing through chromatin-level regulation. Mol. Cell *32*, 232–246.

Pasini, D., Bracken, A.P., Hansen, J.B., Capillo, M., and Helin, K. (2007). The polycomb group protein Suz12 is required for embryonic stem cell differentiation. Mol. Cell. Biol. *27*, 3769–3779.

Pasini, D., Cloos, P.A., Walfridsson, J., Olsson, L., Bukowski, J.P., Johansen, J.V., Bak, M., Tommerup, N., Rappsilber, J., and Helin, K. (2010). JARID2 regulates binding of the Polycomb repressive complex 2 to target genes in ES cells. Nature *464*, 306–310.

Patnaik, D., Chin, H.G., Estève, P.O., Benner, J., Jacobsen, S.E., and Pradhan, S. (2004). Substrate specificity and kinetic mechanism of mammalian G9a histone H3 methyltransferase. J. Biol. Chem. *279*, 53248–53258.

Peng, J.C., Valouev, A., Swigut, T., Zhang, J., Zhao, Y., Sidow, A., and Wysocka, J. (2009). Jarid2/Jumonji coordinates control of PRC2 enzymatic activity and target gene occupancy in pluripotent cells. Cell *139*, 1290–1302.

Pereira, C.F., Piccolo, F.M., Tsubouchi, T., Sauer, S., Ryan, N.K., Bruno, L., Landeira, D., Santos, J., Banito, A., Gil, J., et al. (2010a). ESCs require PRC2 to direct the successful reprogramming of differentiated cells toward pluripotency. Cell Stem Cell *6*, 547–556.

Pereira, J.D., Sansom, S.N., Smith, J., Dobenecker, M.W., Tarakhovsky, A., and Livesey, F.J. (2010b). Ezh2, the histone methyltransferase of PRC2, regulates the balance between self-renewal and differentiation in the cerebral cortex. Proc. Natl. Acad. Sci. USA *107*, 15957–15962.

Rathert, P., Dhayalan, A., Murakami, M., Zhang, X., Tamas, R., Jurkowska, R., Komatsu, Y., Shinkai, Y., Cheng, X., and Jeltsch, A. (2008). Protein lysine methyltransferase G9a acts on non-histone targets. Nat. Chem. Biol. *4*, 344–346.

Roopra, A., Qazi, R., Schoenike, B., Daley, T.J., and Morrison, J.F. (2004). Localized domains of G9a-mediated histone methylation are required for silencing of neuronal genes. Mol. Cell *14*, 727–738.

Sampath, S.C., Marazzi, I., Yap, K.L., Sampath, S.C., Krutchinsky, A.N., Mecklenbräuker, I., Viale, A., Rudensky, E., Zhou, M.M., Chait, B.T., and Tarakhovsky, A. (2007). Methylation of a histone mimic within the histone methyltransferase G9a regulates protein complex assembly. Mol. Cell *27*, 596–608.

Schaefer, A., Sampath, S.C., Intrator, A., Min, A., Gertler, T.S., Surmeier, D.J., Tarakhovsky, A., and Greengard, P. (2009). Control of cognition and adaptive behavior by the GLP/G9a epigenetic suppressor complex. Neuron *64*, 678–691.

Schoeftner, S., Sengupta, A.K., Kubicek, S., Mechtler, K., Spahn, L., Koseki, H., Jenuwein, T., and Wutz, A. (2006). Recruitment of PRC1 function at the initiation of X inactivation independent of PRC2 and silencing. EMBO J. *25*, 3110–3122.

Shen, X., Liu, Y., Hsu, Y.J., Fujiwara, Y., Kim, J., Mao, X., Yuan, G.C., and Orkin, S.H. (2008). EZH1 mediates methylation on histone H3 lysine 27 and complements EZH2 in maintaining stem cell identity and executing pluripotency. Mol. Cell *32*, 491–502.

Shirato, H., Ogawa, S., Nakajima, K., Inagawa, M., Kojima, M., Tachibana, M., Shinkai, Y., and Takeuchi, T. (2009). A jumonji (Jarid2) protein complex represses cyclin D1 expression by methylation of histone H3-K9. J. Biol. Chem. *284*, 733–739.

Simon, J.A., and Kingston, R.E. (2013). Occupying chromatin: Polycomb mechanisms for getting to genomic targets, stopping transcriptional traffic, and staying put. Mol. Cell *49*, 808–824.

Tachibana, M., Sugimoto, K., Fukushima, T., and Shinkai, Y. (2001). Set domain-containing protein, G9a, is a novel lysine-preferring mammalian histone methyltransferase with hyperactivity and specific selectivity to lysines 9 and 27 of histone H3. J. Biol. Chem. *276*, 25309–25317.

Tachibana, M., Ueda, J., Fukuda, M., Takeda, N., Ohta, T., Iwanari, H., Sakihama, T., Kodama, T., Hamakubo, T., and Shinkai, Y. (2005). Histone methyltransferases G9a and GLP form heteromeric complexes and are both crucial for methylation of euchromatin at H3-K9. Genes Dev. *19*, 815–826.

Tachibana, M., Matsumura, Y., Fukuda, M., Kimura, H., and Shinkai, Y. (2008). G9a/GLP complexes independently mediate H3K9 and DNA methylation to silence transcription. EMBO J. *27*, 2681–2690.

Tsukada, Y., Ishitani, T., and Nakayama, K.I. (2010). KDM7 is a dual demethylase for histone H3 Lys 9 and Lys 27 and functions in brain development. Genes Dev. *24*, 432–437.

Voigt, P., LeRoy, G., Drury, W.J., 3rd, Zee, B.M., Son, J., Beck, D.B., Young, N.L., Garcia, B.A., and Reinberg, D. (2012). Asymmetrically modified nucleosomes. Cell *151*, 181–193.

Wang, Z., Zang, C., Rosenfeld, J.A., Schones, D.E., Barski, A., Cuddapah, S., Cui, K., Roh, T.Y., Peng, W., Zhang, M.Q., and Zhao, K. (2008). Combinatorial patterns of histone acetylations and methylations in the human genome. Nat. Genet. *40*, 897–903.

Whyte, W.A., Bilodeau, S., Orlando, D.A., Hoke, H.A., Frampton, G.M., Foster, C.T., Cowley, S.M., and Young, R.A. (2012). Enhancer decommissioning by LSD1 during embryonic stem cell differentiation. Nature *482*, 221–225.

Wu, H., Chen, X., Xiong, J., Li, Y., Li, H., Ding, X., Liu, S., Chen, S., Gao, S., and Zhu, B. (2011). Histone methyltransferase G9a contributes to H3K27 methylation in vivo. Cell Res. *21*, 365–367.

Yuan, P., Han, J., Guo, G., Orlov, Y.L., Huss, M., Loh, Y.H., Yaw, L.P., Robson, P., Lim, B., and Ng, H.H. (2009). Eset partners with Oct4 to restrict extraembryonic trophoblast lineage potential in embryonic stem cells. Genes Dev. *23*, 2507–2520.

Zentner, G.E., and Henikoff, S. (2013). Regulation of nucleosome dynamics by histone modifications. Nat. Struct. Mol. Biol. *20*, 259–266.

Zhang, Y., Yang, X., Gui, B., Xie, G., Zhang, D., Shang, Y., and Liang, J. (2011). Corepressor protein CDYL functions as a molecular bridge between polycomb repressor complex 2 and repressive chromatin mark trimethylated histone lysine 27. J. Biol. Chem. *286*, 42414–42425.

Zheng, D., Zhao, K., and Mehler, M.F. (2009). Profiling RE1/REST-mediated histone modifications in the human genome. Genome Biol. *10*, R9.